

## Observation of Non-Phase-Matched Parametric Amplification in Resonant Nonlinear Optics

Stéphane Coen,<sup>1,2</sup> David A. Wardle,<sup>1</sup> and John D. Harvey<sup>1</sup>

<sup>1</sup>*Physics Department, The University of Auckland, Private Bag 92019, Auckland, New Zealand*

<sup>2</sup>*Optics and Acoustics, Université Libre de Bruxelles, Avenue F.D. Roosevelt 50, CP 194/5, B-1050 Brussels, Belgium*

(Received 8 July 2002; published 13 December 2002)

The coupling between a resonant excitation and a nonresonant parametric process in a nonlinear system is studied experimentally under non-phase-matched conditions. Our study performed in the context of anti-Stokes stimulated Raman scattering provides a clear observation of the self-induced phase matching of a parametric process. A close agreement with theoretical predictions is observed.

DOI: 10.1103/PhysRevLett.89.273901

PACS numbers: 42.65.Dr, 42.65.Hw, 42.65.Sf, 42.81.-i

The intimate coupling between resonant excitation and nonresonant parametric processes in nonlinear systems is well known to lead to unexpected results. This was first revealed in the seminal theoretical work of Bloembergen and Shen on stimulated Raman scattering (SRS) [1], in the context of nonlinear optics. These authors predicted the suppression of the medium excitation and the disappearance of the SRS gain under conditions corresponding to the phase matching of the parametric process associated with the optical waves involved in the resonant Raman interaction. Experiments have been shown to be in excellent agreement with these predictions [1,2]. The suppression of multiphoton ionization by third harmonic generation [3] and the suppression of amplified spontaneous emission by four-wave mixing [4] are two other examples of nonlinear systems exhibiting similar behaviors. As a matter of fact, the quenching of a resonant nonlinearity in physical situations where a competition exists with a nonresonant process has been demonstrated to be a general feature of nonlinear optics [5,6].

So far, the experimental study of these coupled nonlinear effects has been somewhat restricted to the strong coupling regime, i.e., to small values of the linear phase mismatch of the associated nonresonant parametric process. Unexpected results also arise, however, when the phase mismatch is large and when the resonant and nonresonant effects are *a priori* decoupled. In this Letter, we investigate experimentally a system whose basic dynamical behavior is dominated by such weakly coupled nonlinear effects. More specifically, we analyze the unexpected amplification of the anti-Stokes wave in the SRS process, a phenomenon whose description constitutes another result of Bloembergen and Shen's theory [1]. SRS is characterized by the stimulated conversion of photons from an intense optical pump wave into lower frequency Stokes photons through the resonant excitation of a vibration in the transmission medium. The opposite process in which pump photons are converted into up-shifted anti-Stokes photons is also possible when combined with medium deexcitation. We note that the resonant nature of SRS is due to the fact that the beating

frequency between the pump and the Stokes (anti-Stokes) wave matches a vibrational transition of the medium [1,2,6]. The SRS gain typically exhibits an asymmetric profile: Only the down-shifted Stokes waves are amplified while the up-shifted anti-Stokes waves are exponentially absorbed. The unavoidable parametric coupling between the optical waves leads, however, to the exponential amplification of the anti-Stokes wave, even under non-phase-matched conditions [1]. Accordingly, although a simple theory of SRS predicts that the amplified wave has a pure Stokes character, a slight admixture at the anti-Stokes frequency is in practice always present. This explains the unexpectedly high levels of anti-Stokes radiation observed in many experiments [7–9]. In the following, we provide for the first time a direct quantitative observation of this phenomenon.

To ensure a good understanding of our experimental observations, let us recall briefly the theoretical results of Bloembergen and Shen [1]. In the following, we assume that the nonlinear medium is a single-mode silica fiber as in our experiments. The use of a single-mode fiber waveguide enables one to make observations unhampered by the diffraction of the beams and to realize the regime of plane wave interaction assumed in the theory. Silica fibers exhibit a  $\chi^{(3)}$  Kerr nonlinearity that mainly stems from the instantaneous anharmonic motion of bound electrons under the influence of an applied field [8]. SRS arises due to the additional excitation of internal vibrational modes of the silica molecules and can be represented as a delayed contribution to the nonlinearity [8,10]. In these conditions, the combined effect of parametric four-wave mixing and SRS can be described by a generalized nonlinear Schrödinger equation (GNLSE) [8] that reads

$$\frac{\partial A(z, t)}{\partial z} = -i \frac{\beta_2}{2} \frac{\partial^2 A(z, t)}{\partial t^2} + i\gamma \left[ (1-f)|A(z, t)|^2 + f \int_{-\infty}^t \chi_R^{(3)}(t-t') |A(z, t')|^2 dt' \right] A(z, t). \quad (1)$$

Here  $A(z, t)$  is the envelope of the electric field,  $z$  is the longitudinal coordinate along the fiber axis, while  $t$  is the time in a reference frame traveling at the group velocity of light in the fiber.  $\beta_2$  and  $\gamma$  are, respectively, the dispersion and the nonlinearity coefficients of the fiber.  $\chi_R^{(3)}(t)$  is the inverse Fourier transform of the complex Raman susceptibility  $\tilde{\chi}_R^{(3)}(\Omega)$ , and  $f \simeq 0.18$  measures the fractional contribution of the Raman susceptibility to the instantaneous Kerr effect [ $\tilde{\chi}_R^{(3)}(0) = 1$ ] [10].

The coupled evolution of the Raman Stokes and anti-Stokes waves can be investigated in the undepleted pump approximation by introducing in the GNLSE (1) the ansatz  $A(z, t) = [\sqrt{P_p} + A_s(z) \exp(i\Omega t) + A_a(z) \exp(-i\Omega t)] \exp(i\gamma P_p z)$ . In this expression,  $P_p$  is the pump power while  $A_\alpha(z) = \sqrt{P_\alpha(z)} \exp[i\phi_\alpha(z)]$  ( $\alpha = s, a$ ) are the amplitudes of the Stokes and the anti-Stokes waves,  $P_\alpha(z)$  and  $\phi_\alpha(z)$  representing, respectively, the power and the phase of these two waves.  $\Omega = \omega_p - \omega_s = \omega_a - \omega_p$  is the angular frequency shift between the pump and the Stokes/anti-Stokes waves ( $\Omega > 0$ ). At first order in the amplitudes of the Stokes and anti-Stokes waves  $A_s$  and  $A_a$ , we obtain the linear problem

$$\frac{d}{dz} \begin{bmatrix} A_s \\ A_a^* \end{bmatrix} = i \begin{bmatrix} \gamma q P_p + \Delta k/2 & \gamma q P_p \\ -\gamma q P_p & -\gamma q P_p - \Delta k/2 \end{bmatrix} \begin{bmatrix} A_s \\ A_a^* \end{bmatrix}, \quad (2)$$

with  $q = 1 - f + f\tilde{\chi}_R^{(3)}(-\Omega)$  and where  $\Delta k = \beta_2 \Omega^2$  is the linear phase mismatch between the three waves. In the limit where  $\Delta k$  is large in comparison to the nonlinear contribution to the mismatch,  $|\Delta k| \gg |2\gamma q P_p|$ , Eqs. (2) reveal the existence of an exponentially growing mode with an almost pure Stokes character, which corresponds to the growing of the Stokes wave under the influence of SRS. However, because of four-wave mixing [represented by the off-diagonal terms in Eqs. (2)], this mode is always partially anti-Stokes. The ratio between the two components of the growing mode is given by

$$\frac{A_a^*}{A_s} \simeq \frac{-\gamma q P_p}{2\gamma q P_p + \Delta k} \simeq \frac{-\gamma q P_p}{\Delta k}. \quad (3)$$

This well known equation [1,2,11] clearly shows the four-wave-mixing mediated coupling that exists between the anti-Stokes and the Stokes waves. We note that it is valid both in the normal and in the anomalous dispersion regime, as long as the linear phase mismatch is large. Equation (3) indicates that the anti-Stokes power  $P_a = |A_a|^2$  is going to grow along the fiber in proportion to  $P_p^2 P_s(z) \propto P_p^2 \exp(g P_p z)$ . Here  $g \simeq g_s$  is the power gain of the growing mode, which is close to the pure SRS gain  $g_s = -2\gamma \Im(q)$  normally seen by the Stokes wave in the absence of four-wave mixing. So, while SRS normally results in an exponential absorption of the anti-Stokes wave, the weak coupling that exists between SRS and four-wave mixing actually leads to the amplification of that wave with a power gain close to the pure SRS Stokes gain  $g_s$ . Equation (3) also reveals that propagation is such

that  $\Delta\phi = \phi_s + \phi_a$  remains constant. As this phase parameter acts as a control value for the efficiency and the sign of the parametric energy transfer between the pump and the Stokes/anti-Stokes waves [8], its stationarity indicates that the Stokes and anti-Stokes waves are phase matched with the pump, despite the large linear phase mismatch. The parametric coupling between the three waves involved in the resonant Raman interaction is thus able to self-induce the phase matching so that the anti-Stokes wave undergoes a net positive parametric gain along the whole fiber [9].

To understand how phase matching is self-induced, we have performed a numerical integration of the amplitude equations (2) with a large linear phase mismatch. A typical result is plotted in Fig. 1 that shows the evolution of (a) the Stokes and anti-Stokes powers  $P_s$  and  $P_a$  and (b) the phase parameter  $\Delta\phi$ . This figure can be interpreted by examining the equations governing the evolution of these variables as the field propagates along the fiber and that can be derived from Eqs. (2),

$$dP_s/dz = [+g_s - 2\gamma\sqrt{P_a/P_s}\Im(qe^{-i\Delta\phi})]P_p P_s, \quad (4)$$

$$dP_a/dz = [-g_s + 2\gamma\sqrt{P_s/P_a}\Im(qe^{+i\Delta\phi})]P_p P_a, \quad (5)$$

$$d\Delta\phi/dz = \Delta k + \gamma P_p [2(1-f) + \Re(q\sqrt{P_a/P_s}e^{-i\Delta\phi} + q\sqrt{P_s/P_a}e^{i\Delta\phi})]. \quad (6)$$

Here the influence of four-wave mixing on the coupled-wave dynamics appears in the form of terms depending on  $\exp(\pm i\Delta\phi)$ . In particular, it is clearly apparent how the pure Raman gain (loss)  $\pm g_s$  seen by the Stokes (anti-Stokes) waves is modified by four-wave mixing.

Since we consider the case where  $|\Delta k| \gg |2\gamma q P_p|$ , the linear phase mismatch  $\Delta k$  initially dominates the right-hand side of Eq. (6). In the first stage of propagation,  $\Delta\phi$  therefore increases linearly with the propagation distance [left side of Fig. 1(b)], which results, on average, in a cancellation of the contribution of parametric four-wave mixing. In that situation, the coupled-wave dynamics is

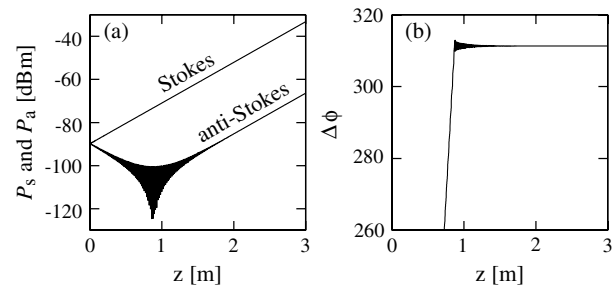


FIG. 1. Typical evolution of (a) the Stokes/anti-Stokes power and (b) phase parameter  $\Delta\phi$ . The pump power is  $P_p = 400$  W and we have set  $P_s(0) = P_a(0) = 1$  nW. All the other parameters are the same as in the experiment.

driven by pure SRS, leading to an exponential increase (decrease) of the Stokes (anti-Stokes) wave, respectively [left side of Fig. 1(a)]. The Stokes to anti-Stokes power ratio  $P_s/P_a$  increases accordingly.

Equations (4)–(6) reveal, however, that the magnitude of the four-wave mixing terms scales with the  $P_s/P_a$  power ratio. As this ratio increases, the nature of the interaction between the three waves changes dramatically. This explains the growing amplitude of the parametric oscillations seen in the evolution of the anti-Stokes power in Fig. 1(a). Moreover, once  $P_s/P_a$  exceeds a certain threshold, a value of  $\Delta\phi$  exists for which the nonlinear induced phase shift represented by the second term of Eq. (6) is sufficiently large to compensate for the linear phase mismatch  $\Delta k$ . From that point,  $\Delta\phi$  steadies and becomes fixed and four-wave mixing is able to amplify the anti-Stokes wave. This transition is clearly seen near  $z = 1$  m in Fig. 1. However, by transferring the same amount of power from the pump to the Stokes and anti-Stokes waves, four-wave mixing not only results in the amplification of these two waves but also in the decrease of the  $P_s/P_a$  power ratio. Therefore, after a short transient, SRS and four-wave mixing balance each other so that both sidebands are amplified with the same gain while  $P_s/P_a$  and  $\Delta\phi$  remain constant (right part of Fig. 1). The Stokes wave is mainly amplified through SRS whereas the anti-Stokes wave follows the evolution of the Stokes wave through parametric amplification. Phase-matching is self-induced thanks to the SRS-induced power imbalance between the two sidebands.

To perform a detailed experimental study of the coupled Stokes/anti-Stokes dynamics under non-phase-matched conditions, we have used a conceptually simple setup. The pump source was a mode-locked, cavity dumped krypton ion laser that emits 60 ps (FWHM)  $\text{sech}^2$ -shaped pulses at the wavelength  $\lambda = 647.1$  nm with a repetition rate of 1.176 MHz. These pulses were launched along the fast axis of a 2.85-m-long single-mode polarization-maintaining (PM) silica fiber ( $\Delta n \approx 5 \times 10^{-5}$ ). With this arrangement, no pure four-wave-mixing processes are phase matched under our experimental conditions. At the output end of the fiber, a polarizing beam splitter was used to select the radiation copropagating with, and polarized parallel to, the pump. This light beam was then dispersed by a triple prism monochromator and the time-averaged power per unit angular frequency  $\Gamma$  was measured by a calibrated photomultiplier tube operated in the photon counting regime. In practice, the measurements were performed with a frequency shift corresponding to the peak of the Raman gain of silica,  $\Omega/(2\pi) = 13.2$  THz, for which we have  $\tilde{\chi}_R^{(3)}(-\Omega) = -1.38i$  [10]. As regards the fiber parameters, the effective area of the fiber was measured with a far-field scanning technique,  $A_{\text{eff}} \approx 13.5 \mu\text{m}^2$ , which has allowed us to evaluate the fiber nonlinearity coefficient,  $\gamma = 2\pi n_2/(\lambda A_{\text{eff}}) \approx 23/(\text{W km})$ , where  $n_2 = 3.2 \times 10^{-20} \text{ m}^2/\text{W}$  is the nonlinear refractive

index of silica [8]. We were not able to measure the fiber dispersion coefficient  $\beta_2$ , but we can reasonably assume that, at our pump wavelength, the fiber dispersion is close to the dispersion of pure silica,  $\beta_2 \approx 50 \text{ ps}^2/\text{km}$  [8]. With this dispersion, we have a large linear phase mismatch,  $\Delta k \approx 350 \text{ m}^{-1}$ , while the walk-off between the three waves is reasonably small.

The experimental measurements presented in Fig. 2 show how the spectral intensities of the Stokes and anti-Stokes waves vary with the pump power. Three dynamical regimes can be identified. For low values of the pump power, Raman scattering is mainly spontaneous so that the power of both the Stokes and the anti-Stokes waves increases linearly with the pump. Note that these parts of the curves are not reproduced by the theoretical model Eqs. (2) because it does not include spontaneous scattering. When the sidebands have grown sufficiently, stimulated scattering becomes the dominant process. Accordingly, a transition to an exponential growing regime is observed for the Stokes wave while the anti-Stokes power saturates as the spontaneous emission rate is balanced by the stimulated absorption rate. Eventually, for sufficiently large values of the pump power, an abrupt transition in the evolution of the anti-Stokes power is observed. At this stage, self-induced phase matching is achieved and the parametric gain enters into play. This occurs when the Stokes power becomes sufficiently large that the predicted anti-Stokes power derived from Eq. (3) exceeds the spontaneous anti-Stokes noise background. A dramatic increase is then observed for the anti-Stokes wave, whose power appears to be a faster growing function of the pump power than the Stokes power, in good agreement with the theoretical predictions.

For a better comparison of our experimental results with the coupled-wave theory, we have plotted in Fig. 3 the value of  $r = (1/P_p)\sqrt{P_a/P_s}$  calculated for the experimental data. According to Eq. (3), this expression should be a constant equal to  $|\gamma q/(\beta_2 \Omega^2)| \approx 5.8 \times 10^{-5}/\text{W}$  in

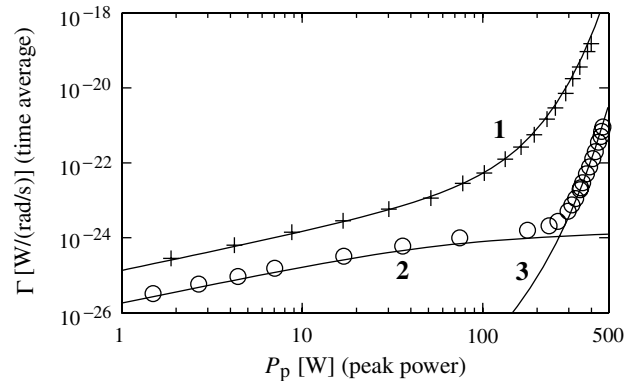


FIG. 2. Experimental time-averaged scattered power per unit angular frequency versus the pump power for the Stokes (crosses) and anti-Stokes (circles) waves. The solid lines labeled 1, 2, 3 are the analytical predictions.

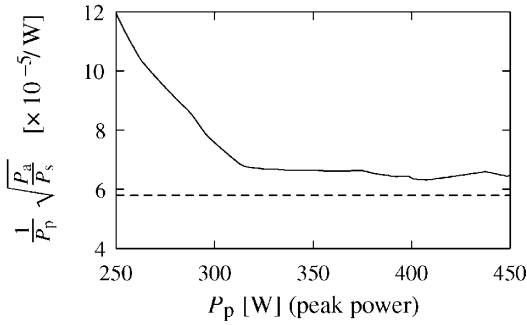


FIG. 3. Evolution of  $(1/P_p)\sqrt{P_a/P_s}$  for the experimental data (solid line). The dashed line is the theoretical prediction.

the regime where four-wave mixing is effectively phase matched. As can be seen in Fig. 3, the experimental value of  $r$  plateaus to the value of  $\sim 6.6 \times 10^{-5}/W$  which, given the uncertainties in  $\beta_2$  and  $\gamma$ , is remarkably close to the theoretical prediction. We must also note in Fig. 3 that the transition between the pure SRS regime and the regime where SRS and four-wave mixing become closely coupled appears remarkably clear.

The ability of Eq. (3) to predict accurately the ratio between the Stokes and the anti-Stokes power has also made possible a complete analytical fit of the experimental data. To this end, we have used Eq. (3) together with a model describing the combined influence of spontaneous and stimulated Raman scattering (and excluding four-wave mixing) [10,12,13],

$$\Gamma_\alpha(P_p) = \frac{\omega_\alpha R_\alpha}{\omega_p g_\alpha} [e^{g_\alpha L P_p} - 1], \quad (7)$$

$$g_\alpha = \frac{4\pi}{\hbar\omega_p} \frac{R_\alpha}{1 \pm \coth[\hbar\Omega/(2k_B T)]}, \quad (8)$$

$$\frac{R_s}{R_a} \approx \left(\frac{\omega_s}{\omega_a}\right)^2 e^{\hbar\Omega/(k_B T)}. \quad (9)$$

In the above expressions,  $\alpha = s, a$ ,  $L$  is the fiber length,  $k_B$  is the Boltzmann constant,  $T \approx 293$  K is the fiber temperature, and the plus sign (minus sign) in the expression of the Raman gain  $g_\alpha$  corresponds to the Stokes (anti-Stokes) wave, respectively. The Raman gain coefficients  $g_\alpha$  are related to the spontaneous emission rates  $R_\alpha$  by Eqs. (8) [10]. Moreover, the spontaneous emission rates for the Stokes and anti-Stokes waves are not independent; see Eq. (9) [13]. Consequently, there is only one free parameter. This has been taken as  $R_s \approx 5.97 \times 10^{-22} \text{ m}^{-1}(\text{rad/s})^{-1}$ , a value measured from the slope of the linear part of the experimental Stokes curve.  $\Gamma_s$  and  $\Gamma_a$  can then be calculated. Averaging over the pump pulse profile yields the curves labeled 1 and 2 in Fig. 2. The curve labeled 3, which describes the parametric amplification of the anti-Stokes wave, has then been obtained from  $\Gamma_s$ , combined with Eq. (3), through a similar averaging procedure. As may be seen, the fit is excellent.

In particular, the gain seen by the anti-Stokes wave is correctly reproduced by the theory.

In summary, we have studied experimentally a system whose dynamics is dominated by the weak coupling between a resonant excitation and a nonresonant parametric process under non-phase-matched conditions. More specifically, we have measured quantitatively the evolution of the anti-Stokes wave in the SRS process. Our measurements are found to verify closely the long-standing theoretical results of Bloembergen and Shen [1] and reveal clearly how phase matching can be self-induced in this system despite the weak initial influence of four-wave mixing. Also, our work emphasizes the important role of non-phase-matched waves in wave mixing phenomena [14]. Finally, we note that a large anti-Stokes to Stokes power ratio of nearly 10% has recently been observed in a photonic crystal fiber thanks to its large nonlinearity and reduced dispersion in the visible [15], which opens up new exciting possibilities for up-frequency conversion applications.

The authors acknowledge the support of the New Zealand Foundation for Research Science and Technology. S.C. also acknowledges the support of the Fonds National de la Recherche Scientifique (FNRS, Belgium).

- 
- [1] N. Bloembergen and Y.R. Shen, Phys. Rev. Lett. **12**, 504 (1964); Y.R. Shen and N. Bloembergen, Phys. Rev. **137**, A1787 (1965).
  - [2] E.A. Golovchenko, P.V. Mamyshev, A.N. Pilipetskii, and E.M. Dianov, IEEE J. Quantum Electron. **26**, 1815 (1990).
  - [3] J.C. Miller, R.N. Compton, M.G. Payne, and W.W. Garrett, Phys. Rev. Lett. **45**, 114 (1980); J.H. Glowina and R.K. Sander, Phys. Rev. Lett. **49**, 21 (1982).
  - [4] M.S. Malcuit, D.J. Gauthier, and R.W. Boyd, Phys. Rev. Lett. **55**, 1086 (1985).
  - [5] J. J. Wynne, Phys. Rev. Lett. **52**, 751 (1984).
  - [6] R. Frey, Opt. Commun. **89**, 441 (1992).
  - [7] R. W. Terhune, Bull. Am. Phys. Soc. **8**, 359 (1963).
  - [8] G. P. Agrawal, *Nonlinear Fiber Optics* (Academic Press, San Diego, 2001), 3rd ed.
  - [9] K. Hakuta, M. Suzuki, M. Katsuragawa, and J.Z. Li, Phys. Rev. Lett. **79**, 209 (1997).
  - [10] R.H. Stolen, J.P. Gordon, W.J. Tomlinson, and H.A. Haus, J. Opt. Soc. Am. B **6**, 1159 (1989).
  - [11] S. Trillo and S. Wabnitz, J. Opt. Soc. Am. B **9**, 1061 (1992).
  - [12] D. A. Long, *Raman Spectroscopy* (McGraw-Hill, New York, 1977).
  - [13] B. Crosignani, P. Di Porto, and S. Solimeno, Phys. Rev. A **21**, 594 (1980); D. A. Wardle (private communication).
  - [14] E. Lantz, D. Gindre, H. Maillotte, and J. Monneret, J. Opt. Soc. Am. B **14**, 116 (1997).
  - [15] S. Coen, A. H. L. Chau, R. Leonhardt, J. D. Harvey, J. C. Knight, W. J. Wadsworth, and P. St. J. Russell, J. Opt. Soc. Am. B **19**, 753 (2002).